CHAPTER VIII

PERFORMANCE OF THE EJECTOR:

EFFECTS OF GEOMETRY'S VARIATION

Form the literature review, it was seen that not only the operating conditions, but the geometries of the ejector also affects the performance of the ejector. In this chapter, in order to study the effect of ejector geometries on the performance of the ejector, 4 interested parameters concerning the geometries are as follows:

- the primary nozzle's throat diameter,
- the mixing chamber inlet diameter,
- the length ejector's throat section, and
- the nozzle exit position.

To investigate the influences of each parameter, the ejector was modeled with the different pieces of components. Variations in shape of the ejector were modeled with respect to the dimension of the experimental ejector given in Table 3.2. During the simulation, for each geometry cases, the upstream operating conditions were fixed. Please also note that, the flow structures in this chapter were analyzed when the ejector models were operated in the choke flow mode at the downstream pressure of 0.94 bar (corresponding to the condenser saturation temperature of around 30°C). Similar to the previous chapter, the detail analyses and discussion on the effect of ejector geometries to the flow characteristics and the performance of the R141b ejector are provided in this chapter.

8.1 Effect of Primary Nozzle Throat Diameter

In the simulation, the primary nozzle throat diameter was varied from 2.5 mm. (Nozzle no.2), 2.8 mm. (Nozzle no.1), and 3.2 mm. (Nozzle no.3). Since the ejector's throat diameter was fixed at 8 mm, changing the size of the primary nozzle diameter caused the variation in the area ratio (AR) from 6.25 to 10.24. The primary fluid pressure and the secondary fluid pressure were fixed at the corresponding saturated temperature of 110°C and 5°C, respectively. Once again, referring to Table 3.2, other significant parts of the ejector were modeled from mixing chamber no.1, throat section no.3 and the subsonic diffuser. The primary nozzle exit plane was fixed at a positive NXP of 30 mm. The results are shown in Figure 8.1.

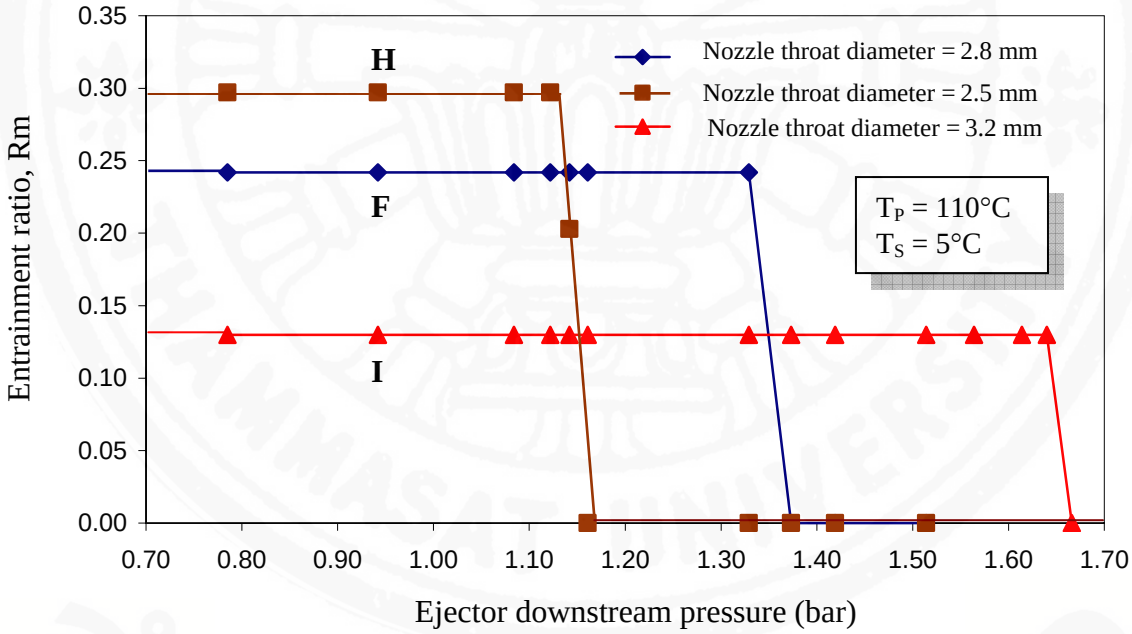

Figure 8.1 Performance characteristics of the R141b ejector, effect of primary nozzle throat diameter.

From Figure 8.1, point H and I, it is seen that when the ejector is equipped with a smaller primary nozzle (H), the entrainment ratio of the ejector can be increased. However, the ejector has to be operated at a lower critical back pressure.

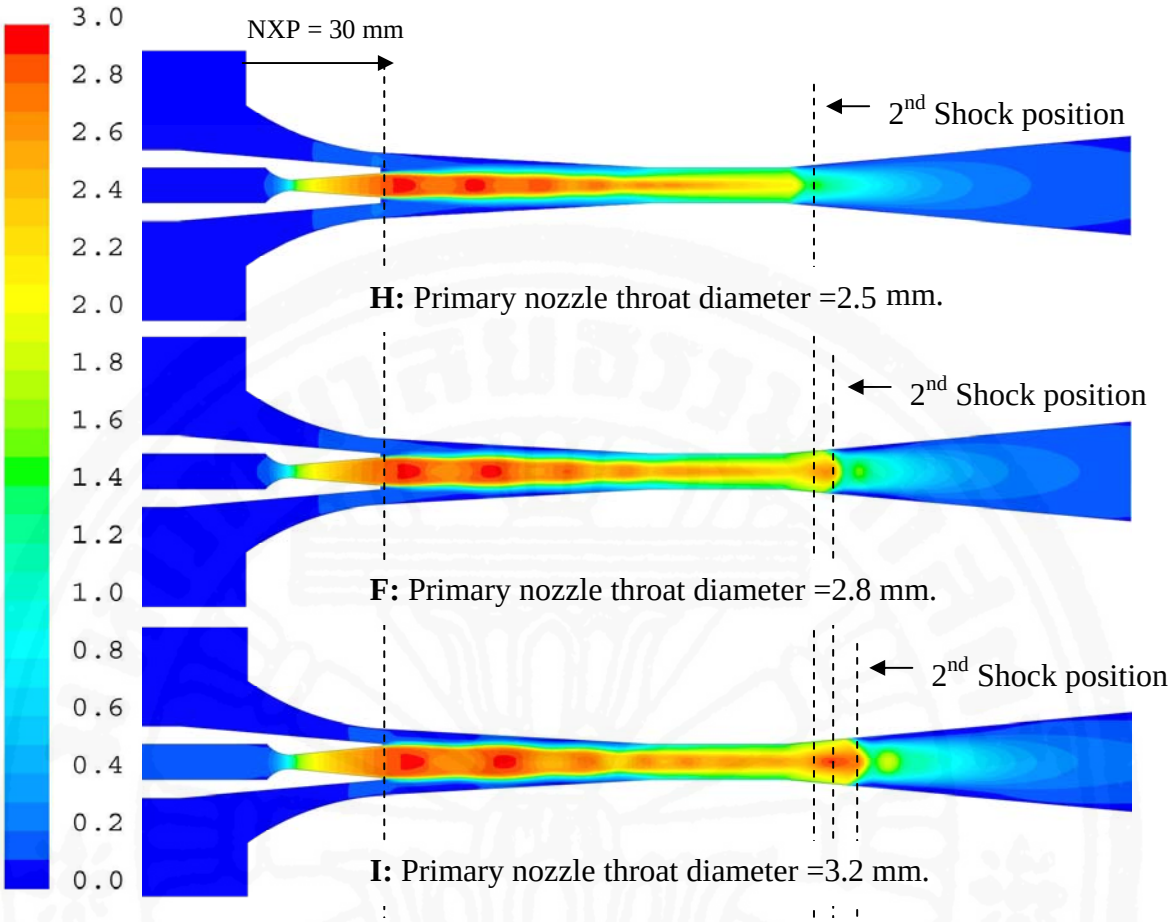

a) Filled contours of Mach number

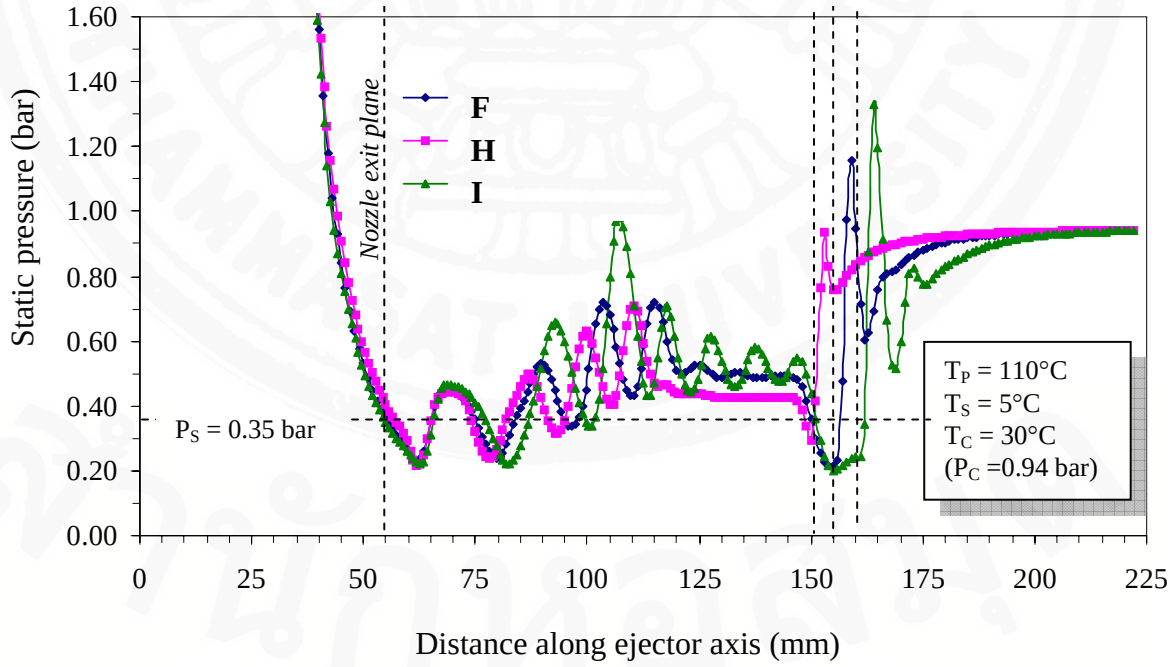

b) Static pressure distribution along the centerline of the ejector

Figure 8.2 Effect of the primary nozzle throat diameter on the flow in the R141b ejector (All operating points, **F**, **H,** and **I**, correspond to those shown in Figure 8.1).

Figure 8.2 shows the contours of Mach number of the ejector simultaneously with the static pressure distributions along the ejector's axis, when its primary nozzle geometry is varied. When the ejector is equipped with a larger primary nozzle, a larger jet core which has higher momentum is produced. Therefore a smaller amount of the secondary fluid is allowed to be entrained through the resultant smaller effective area. On the other hand, the total momentum of the mixed stream increases and a stronger second series of oblique shock can be induced as seen in Figure 8.2b. Consequently, less compression process from the divergent diffuser is needed, and the shocking position moves forward closer to the ejector exit. In conclusion, these flow structures cause a decrease of the entrainment ratio. However, an ejector can be operated at a higher critical back pressure.

8.2 Effect of Mixing Chamber Inlet Diameter

In this case, the simulated domains were modeled with various mixing chamber inlet diameters which were mixing chamber no.1 (inlet diameter = 36 mm.), mixing chamber no.2 (inlet diameter = 12 mm.), and mixing chamber no.3 (inlet diameter = 48 mm.). Other significant parts of the ejector were modeled from, primary nozzle no.1, throat section no.3 and the subsonic diffuser. The primary fluid pressure and the secondary fluid pressure were fixed at the corresponding saturation temperatures of 100°C and 5°C, respectively. The primary nozzle exit plane was fixed at a positive NXP of 30mm. The simulated performance characteristics curves are shown in Figure 8.3.

Figure 8.4a demonstrates the contours of Mach number of the R141b ejector, when its mixing chamber inlet diameter is varied. Obviously, the graphic flow visualization indicates that there is not much effect from the shear mixing and the viscosity of the fluid on the expanded wave.

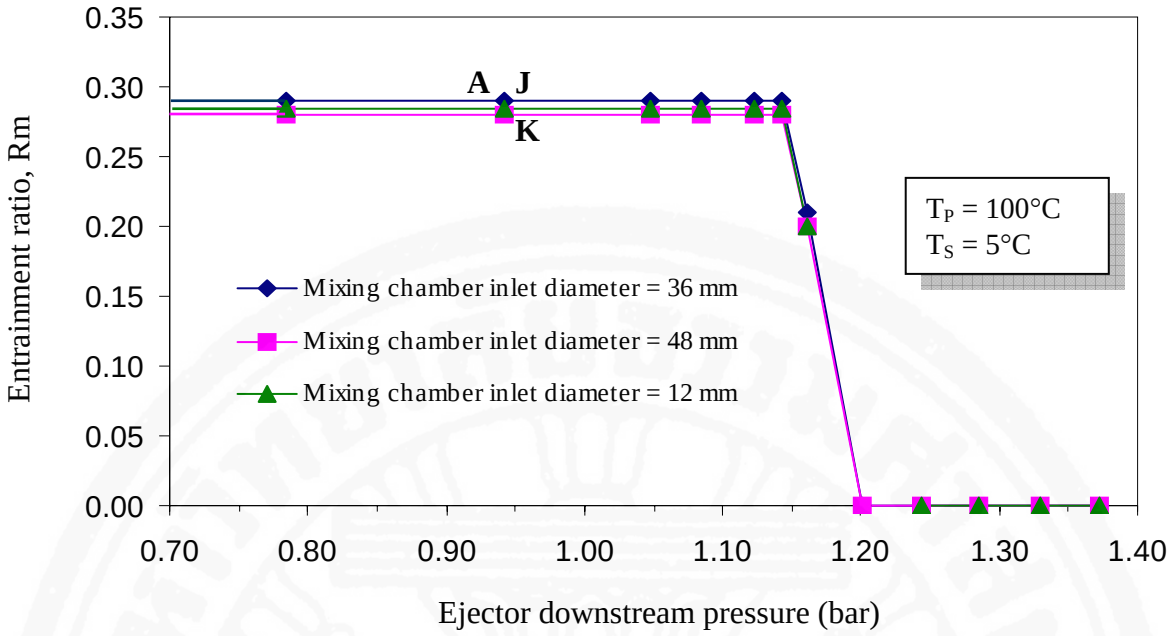

Figure 8.3 Performance characteristics of the R141b ejector, effect of mixing chamber inlet diameter.

The primary jet core of the smaller mixing chamber inlet diameter moves with slightly greater speed and hence higher momentum. On the other hand, entraining the secondary fluid under a slightly higher effect of the shear mixing and the viscosity of the fluid on the expanded wave introduces the higher total pressure loss to the mixed stream. However, as seen from Figure 8.4b, the static pressure profiles along the ejector's axis upstream of the shocking position were almost the same and the shocking position and the critical back pressure of the ejectors were almost unchanged. Moreover, it is seen that the size of jet core and the effective area of the ejectors are similar. Therefore, they can draw the identical amount of secondary fluid, and their entrainment ratios remain the same (Figure 8.3).

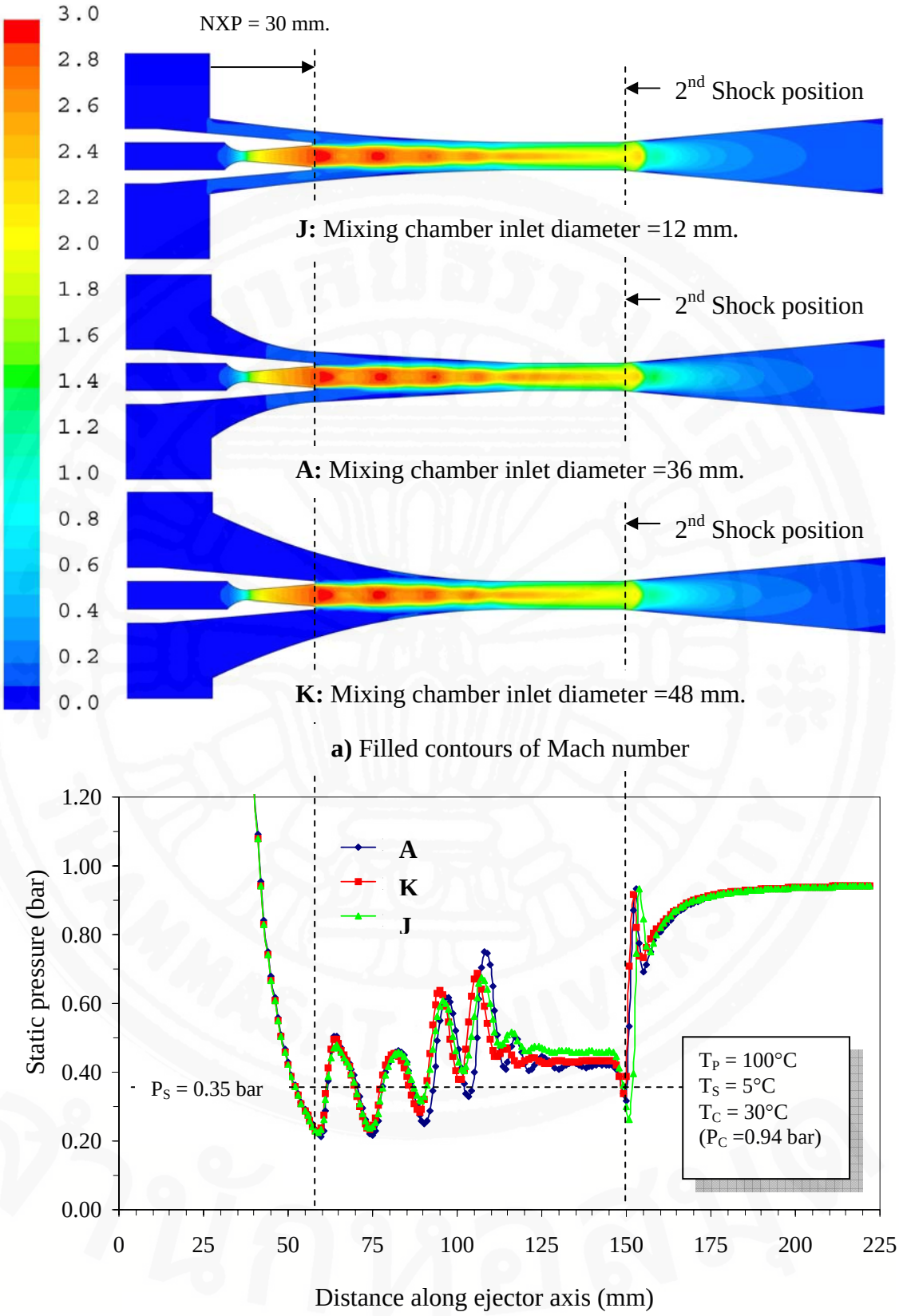

Figure 8.4 Effect of the mixing chamber inlet diameter on the flow in the R141b ejector (All operating points, **A**, **J,** and **K**, correspond to those shown in Figure 8.3).

8.3 Effect of Throat Length

In the simulation, the throat length of the ejector was varied from 16, 32, and 40 mm. The primary fluid pressure and the secondary fluid pressure were fixed at the corresponding saturated temperatures of 100°C and 5°C, respectively. Other significant shapes of the ejector were, for example, the primary nozzle diameter = 2.8 mm, and the NXP = +30 mm. The results of simulated performance are shown in Figure 8.5.

Referring to Figure 8.5, point A, L and M illustrate the performance characteristics of the R141b ejector when its throat length was varied. It is clear that the length of the ejector throat section has almost no influence on the entrainment ratio of the ejector. However, when the ejector is assembled with a longer throat (**M**), the ejector can be operated at a higher critical back pressure.

Figure 8.6 illustrates the graphic flow visualization inside the R141b ejector, when the length of the ejector's throat section is varied.

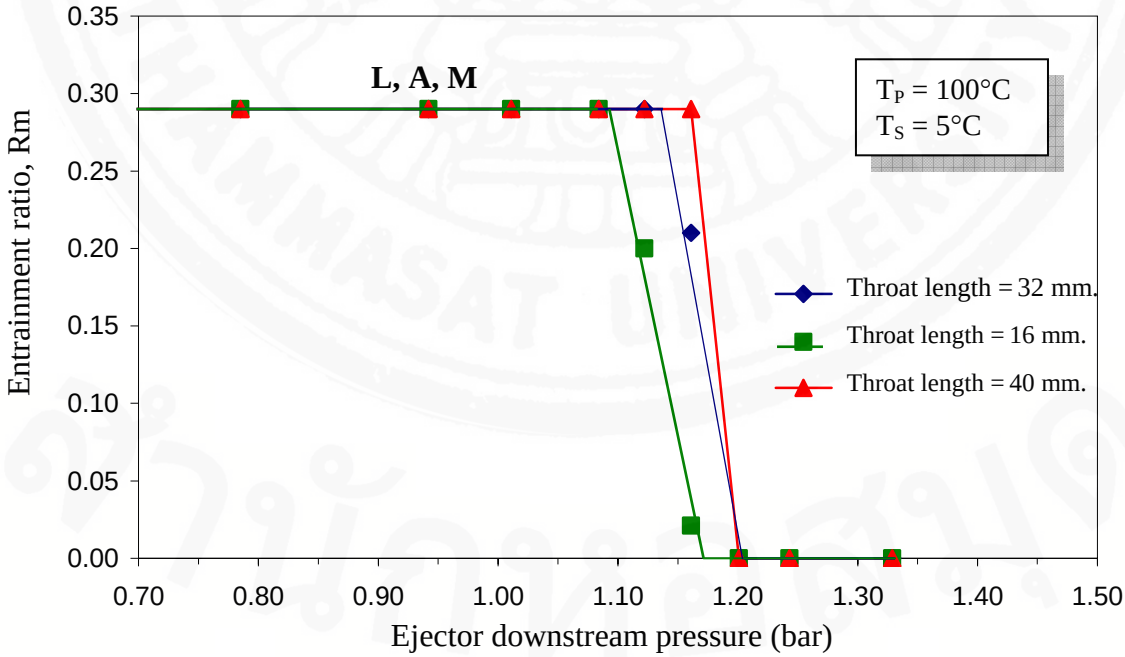

Figure 8.5 Performance characteristics of the R141b ejector, effect of throat length.

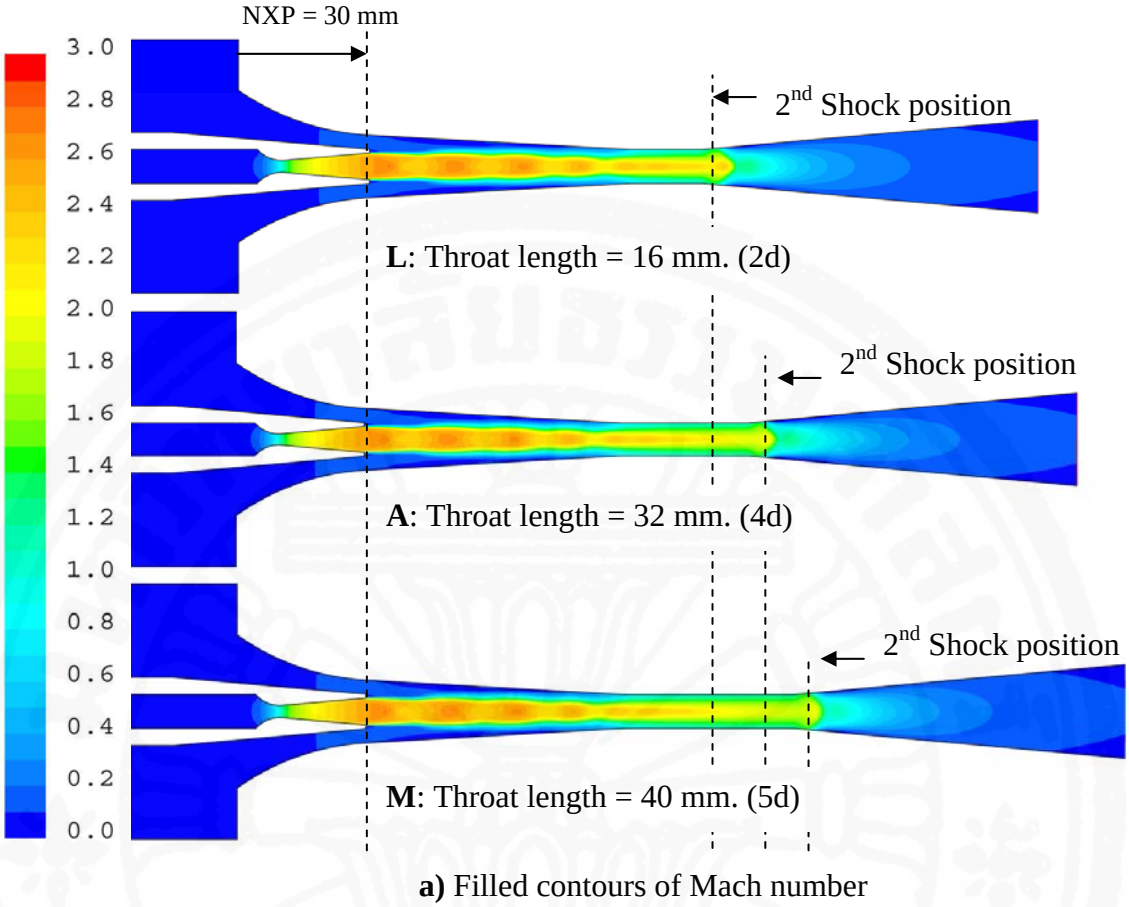

a) Filled contours of Mach number

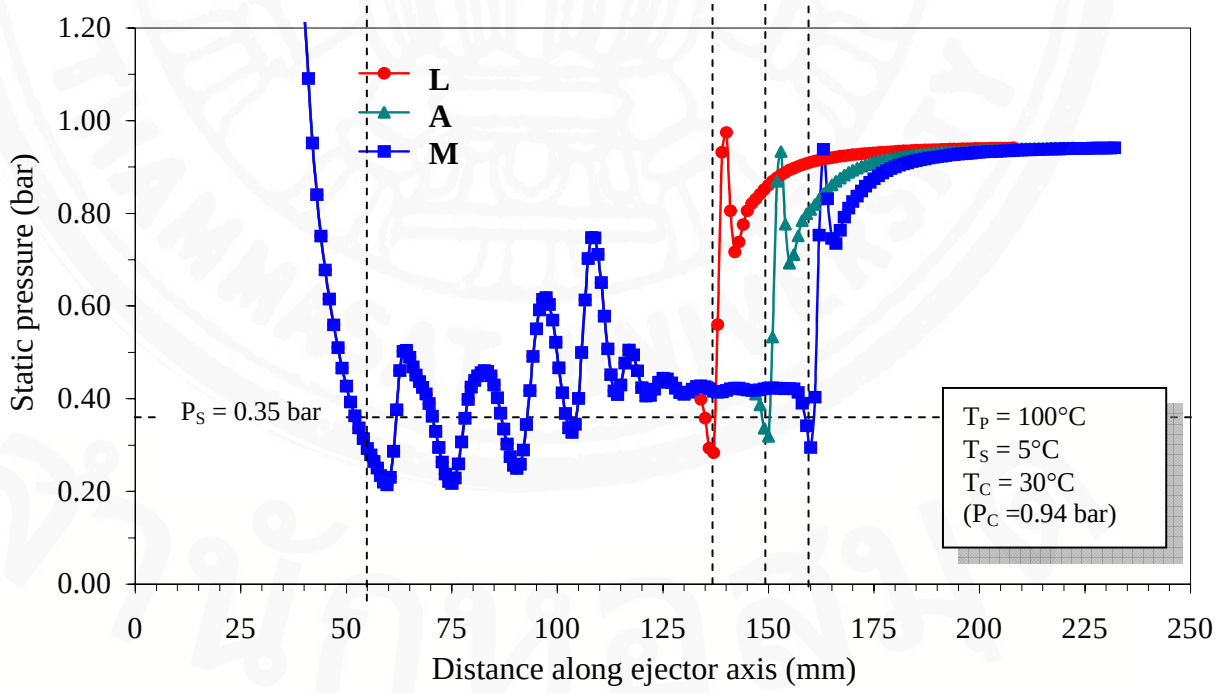

b) Static pressure distribution along the centerline of the ejector

Figure 8.6 Effect of the throat length on the flow in the R141b ejector
(All operating points, **A**, **L,** and **M**, correspond to those shown in Figure 8.5).

It is seen that the length of the ejector throat has almost no influence on the flow structure inside the R141b ejector. These modeled ejectors show the identical sizes of the primary jet core and the expansion angle, thus, resulted in the same size of the effective area. Therefore, the same amount of the secondary fluid can be drawn into the ejector, and consequently the entrainment ratio remains constant.

One interesting point is that the shape of the second series of oblique shock can vary with the length of ejector throat. It is thought that better mixing between the primary jet core and the entrained fluid can be achieved when the longer contact time is provided, as the ejector is fitted with a longer throat section. The better mixing causes the smaller difference between the speed of the primary jet core and the surrounding secondary fluid. Thus the mixed stream becomes more uniform. The induced oblique shock is flattened and a higher compression effect across the shock wave can be achieved, as can be seen in Figure 8.6b.

It can be seen that less compression effect from the divergent portion of a subsonic diffuser is required, and the shocking position moves closer to the diffuser exit. In conclusion, the extended length of the throat section, plus the moving downstream of the shocking position provide a longer distance between the shocking position and the effective area. Therefore, the ejector can be operated at a higher critical back pressure.

However, please note that the elongation of the ejector throat introduces the pressure loss from the interaction of the flow with the viscous boundary layer on the ejector wall. In addition, the reduction of total pressure of the mixed stream is also a result of the induced stronger shock wave. Even though these losses are believed to be small, the accumulated losses from a very long throat and the very strong shock can mitigate the advantage of ejector throat length on the critical point of an ejector.

From the study, it is found that the location of the second shock wave can be varied between the ejector throat and the beginning of the divergent portion of the diffuser. It is determined by the ejector operating conditions which affect the increase of static pressure across the shocking process, plus that in the divergent portion of the subsonic diffuser behind the process. Therefore, in some situation when the shocking position is created in the subsonic diffuser, the supersonic stream is first further accelerated, and its static pressure decreases. However, right after the first shock, its static pressure rebounds and rises to the discharge value.

8.4 Effect of Nozzle Exit Position

In the simulation, only the ejector model constructed with the primary nozzle no.1 was investigated for the effect of various nozzle exit positions. The nozzle exit position (NXP) was varied from positive 20, 30 and 40 mm. The NXP is defined as the distance between the primary nozzle exit plane and the mixing chamber inlet planes. The primary fluid pressure and the secondary fluid pressure were fixed at the corresponding saturated temperatures of 100°C and 5°C, respectively. Other significant shapes of the ejector were, for example, the throat length = 32 mm. (throat no.3), and the mixing chamber inlet diameter = 36 mm. (mixing chamber no.1). The performance curves of the ejector affected by the nozzle exit position are shown in Figure 8.7.

Concerning Figure 8.7, for a given primary fluid and secondary fluid upstream conditions, an entrainment ratio of ejector can be varied when the primary nozzle exit position was placed at the different position. Moving the primary nozzle into the mixing chamber causes the enhancement of both the entrainment ratio and the critical back pressure. Figure 8.8 shows the contours of Mach number of the modeled ejectors, simultaneously with the axis's static pressure distribution, as influenced by the primary

nozzle position. For all cases of different NXP, the primary fluid leaved the primary nozzle's exit in an over-expansion state.

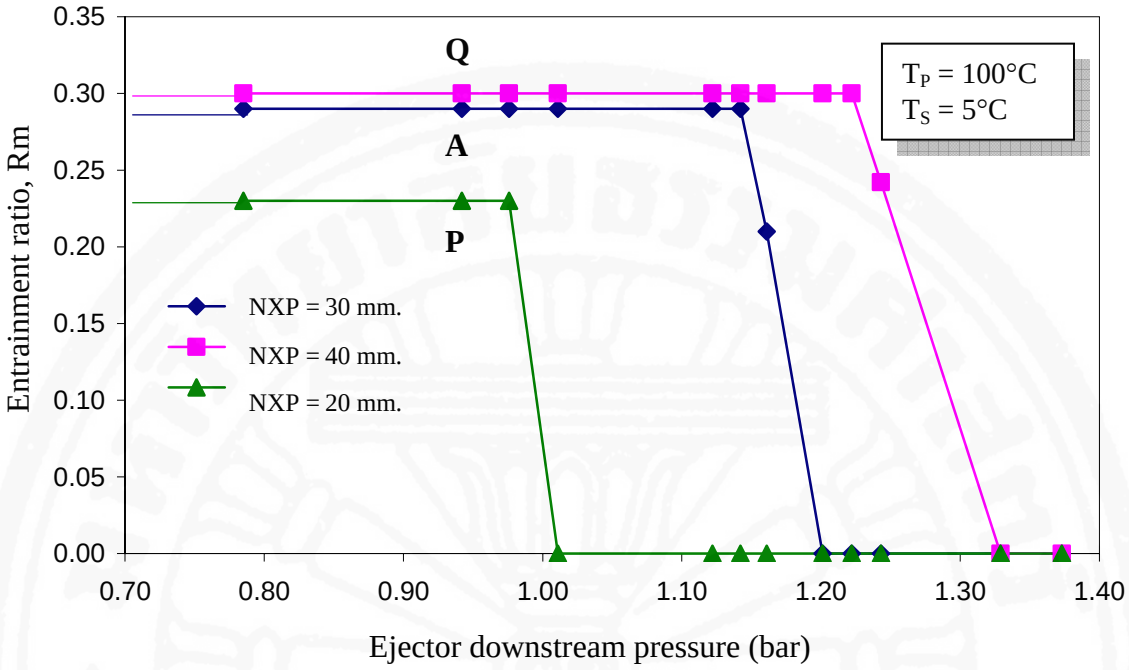

Figure 8.7 Performance characteristics of the R141b ejector, effect of nozzle exit position.

Figure 8.8a shows the contours of Mach number of the modeled ejectors for different primary nozzle positions. The comparison is made at constant condenser pressure of 0.94 bar. At a glance, it can be seen that moving the primary nozzle into the mixing chamber causes a motive fluid to leave the primary nozzle with a smaller expansion angle. According to these changes, the smaller jet core which moves with slightly lower speed and momentum was the result. Thus, there was the larger effective area for the secondary fluid to be entrained through.

From Figure 8.8b, the static pressure profiles along the axis of the ejector, there was an increase of static pressure profiles in the throat section in front of the shocking position, as the primary nozzle was placed closer to the throat section of the ejector. Moreover, moving the nozzle to a higher positive NXP caused the shocking position to slightly move upward closer to the diffuser's end.

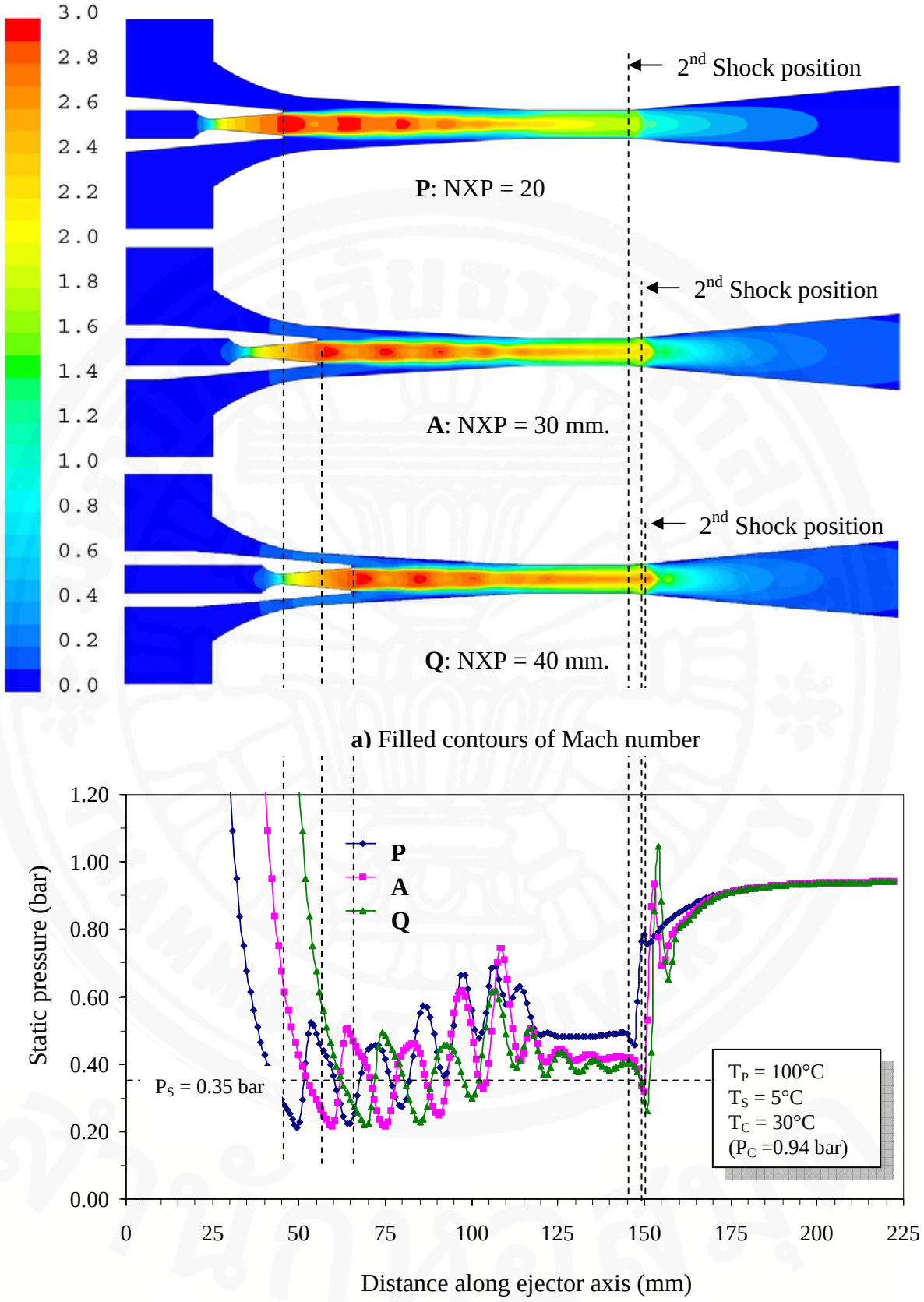

a) Filled contours of Mach number

b) Static pressure distribution along the centerline of the ejector

Figure 8.8 Effect of the nozzle exit position (NXP) on the flow in the R141b ejector (All operating points, **A**, **P,** and **Q**, correspond to those shown in Figure 8.7).

In conclusion, when the primary nozzle was placed downstream into the mixing chamber, the resultant larger effective area allows the primary fluid to entrain a higher rate of secondary fluid into the ejector, thus the higher entrainment ratio is achieved. Moreover, the higher static pressure of the mixed stream in the throat section causes the major increase of its total momentum. Therefore the shocking position moves forward closer to the diffuser's end, and the ejector could be operated at a higher critical condenser pressure.

On the contrary, when the primary fluid leaved the nozzle's exit in an under-expanded state, as normally happened in the case of the steam ejector [39, 40 and 47], retracing out the primary nozzle position off the mixing chamber resulted in a higher entrainment ratio but a lower in the critical back pressure.

8.5 Conclusions

This chapter proposes the theory explaining the flow characteristics reflected the performance of the R141b ejector, when the geometries of the ejector were varied. The change in the flow structure according to the change of the geometries, as visualized using the CFD post-functions, altered the performance of the ejector. It was found that, the change in the performance when the geometries were changed also depended on the primary flow state. At the different primary flow states, the change in the ejector's geometries could affect the change in the flow and the performance of the R141b ejector in different ways as can be concluded in Table 8.1

From Table 8.1, it can be seen that the performance of the R141b ejector, both the entrainment ratio and the critical back pressure, can be improved by moving the nozzle exit position downstream into the mixing chamber when the primary flow state was in an over-expansion state.

Table 8.1 Summarized table for the effect of geometries on the R141b ejector.

Effect Parameters	action	Primary flow state	Performance Characteristic	
			Entrainment ratio **(Rm)**	Critical back pressure **(P_C)**
Effect of Geometry Variations				
Primary nozzle throat diameter	(-)→ (+)	Over-expansion	↓	↑
		Under-expansion		
Mixing chamber inlet diameter	(-)→ (+)	Over-expansion	**unchanged**	**unchanged**
		Under-expansion		
Throat Length	(-)→ (+)	Over-expansion	**unchanged**	↑
		Under-expansion		
NXP	(-)→ (+)	Over-expansion	↑	↑
		Under-expansion	↓	↑

The enhancement of the critical back pressure, but with the decrease in the entrainment ratio could be found, when adjusting the following:

- Increasing the primary nozzle throat diameter.
- Moving the nozzle exit position downstream into the mixing chamber when the primary flow state was at the under-expansion state.

The critical back pressure of an R141b ejector can also be increased by using an ejector with a longer throat section, without the interruption in the amount of the entrained secondary fluid. However, if the throat section is too long, the loss in total pressure may mitigate its advantage on the back pressure which the mixed stream can emit.

Both the entrainment ratio and the critical back pressure were found unchanged, when adjusting the mixing chamber inlet diameter.

In conclusion, this chapter shows the advantage of CFD in investigating the flow mechanisms and the performance of the R141b ejector when operating with various geometries.